Active-Site Specificity of Digestive Aspartic Peptidases from the Four Species of *Plasmodium* that Infect Humans Using Chromogenic Combinatorial Peptide Libraries†

Bret B. Beyer,‡ Jodie V. Johnson,§ Alfred Y. Chung,|| Tang Li,⊥ Amrita Madabushi,‡ Mavis Agbandje-McKenna,‡ Robert McKenna,‡ John B. Dame,⊥ and Ben M. Dunn*,‡

Department of Biochemistry and Molecular Biology, College of Medicine, Department of Chemistry, ICBR Protein Chemistry Core, and Department of Pathobiology, University of Florida, Gainesville, Florida 32610

Received September 29, 2004; Revised Manuscript Received December 6, 2004

ABSTRACT: Two targeted chromogenic octapeptide combinatorial libraries, comprised of 38 pools each containing 361 different peptides, were used to analyze the enzyme/substrate interactions of five plasmepsins. The first library (P1 library) was based on a good synthetic aspartic peptidase substrate [Westling, J., Cipullo, P., Hung, S. H., Saft, H., Dame, J. B., and Dunn, B. M. (1999) *Protein Sci. 8*, 2001−2009; Scarborough, P. E., and Dunn, B. M. (1994) *Protein Eng. 7*, 495−502] and had the sequence Lys-Pro-(Xaa)-Glu-P1*Nph-(Xaa)-Leu. The second library (P1′ library) incorporated results with the plasmepsins from the first library and had the sequence Lys-Pro-Ile-(Xaa)-Nph*P1′-Gln-(Xaa). In both cases, P1 and P1′ were fixed residues for a given peptide pool, where Nph was a *para*-nitrophenylalanine chromogenic reporter and Xaa was a mixture of 19 different amino acids. Kinetic assays monitoring the rates of cleavage of these libraries revealed the optimal P1 and P1′ residues for the five plasmepsins as hydrophobic substitutions. Extended specificity preferences were obtained utilizing liquid chromatography−mass spectrometry (LC−MS) to analyze the cleavage products produced by enzyme-catalyzed digestion of the best pools of each peptide library. LC−MS analysis of the P1-Phe and P1′-Phe pools revealed the favored amino acids at the P3, P2, P2′, and P3′ positions. These analyses have provided new insights on the binding preferences of malarial digestive enzymes that were used to design specific methyleneamino peptidomimetic inhibitors of the plasmepsins. Some of these compounds were potent inhibitors of the five plasmepsins, and their possible binding modes were analyzed by computational methods.

Malaria is a tropical disease found in over 90 countries across the globe, which translates to over 40% of the population of the world living in areas where malaria is endemic. It has been estimated that annually there are between 300 and 500 million clinical cases of malaria worldwide, which results in approximately 2 million deaths (*1*). In recent years, the resistance of both the *Anopheles* mosquito vector and the *Plasmodium* parasites to current methods of control has led to a steady increase in the number of infections and deaths (*1*). Therefore, new antimalarial therapeutic discovery is a critical requirement to decrease worldwide malarial incidence. One possible antimalarial drug target includes peptidases, which are required by the parasite for the metabolism of hemoglobin as a nutrient source or as a mechanism to provide more room for the developing parasite (*2*, *3*).

Malaria, in humans, is a result of an infection by *Plasmodium* parasites of the following species: *P. falciparum* (Pf), *P. vivax* (Pv), *P. malariae* (Pm), and *P. ovale* (Po). While *P. falciparum* is the most deadly form of malaria (*4*), the other three species of parasite also are responsible for the manifestation of the disease. During the intraerythrocytic stage of the life cycle of the parasite, these protozoa consume approximately 75% of the hemoglobin within the infected red blood cells of the host (*3*, *5*). The process of hemoglobin degradation occurs within the acidic food vacuole of the parasite and is catalyzed by aspartic (*6*), cysteine (*7*), and metallopeptidases (*8*). This process appears be an ordered pathway, where it has been postulated that aspartic peptidases may perform the initial steps of hemoglobin cleavage (*4*, *9*). It has been shown that the addition of pepstatin, a specific broad-range aspartic peptidase inhibitor, to cells growing in culture results in the death of the *Plasmodium* parasites (*10*, *11*). These findings provide strong evidence that peptidases are not only involved in essential biological processes of the parasite but also would be putative targets to which antimalarial therapeutics could be designed. Genes encoding aspartic proteases have been cloned from the four human species of *Plasmodium* (*12*).

Synthetic peptide combinatorial techniques have advanced in recent years resulting in the efficient screening of soluble

† This work was supported by NIH Grant AI39211 to J.B.D. and B.M.D. and DK18865 to B.M.D.

* To whom correspondence should be addressed. Telephone: (352) 392-3362. Fax: (352) 846-0412. E-mail: bdunn@ufl.edu.

‡ Department of Biochemistry and Molecular Biology, College of Medicine.

§ Department of Chemistry.

|| ICBR Protein Chemistry Core.

⊥ Department of Pathobiology.

10.1021/bi047886u CCC: $30.25
Published on Web 01/22/2005

substrates to determine peptidase specificity (*13*, *14*). It would be advantageous to use combinatorial methods to probe the substrate preferences of malarial enzymes in the aspartic peptidase family (*15*). In this study, the method detailed by Backes et al. was modified to synthesize libraries of chromogenic peptides, which were used to examine the subsite specificity of five malarial plasmepsins (*16*). In the first library, we have utilized our "best" general substrate for the aspartic peptidase family, Lys-Pro-Ile-Glu-Phe*Nph-Arg-Leu, where the asterisk indicates the expected site of cleavage. Mixtures of amino acids were introduced into two positions, P3 on one side of the cleavage point and P2′ on the other side. A positional scan at P1 was used to establish the "primary" or P1 specificity of the aspartic peptidases. Positions P3 and P2′ were chosen for incorporation of mixtures in the first synthesis because multiple three-dimensional structures of enzyme−ligand complexes have revealed that the side chains in the P3, P1, and P2′ positions are adjacent to each other on the side of the active-site cleft contributed by the amino-terminal domain of the enzyme (*17*). Thus, our strategy was to evaluate the P1 residue preferences of aspartic peptidases in the context of a variety of P3 and P2′ substitutions, which interact with subsites contributed by the N-terminal domain. A second library was designed and synthesized that incorporated the findings from these assays and screened the P2, P1′, and P3′ positions, which interact with subsites on the opposite side of the enzyme active-site cleft. These methods allowed the rapid examination and identification of the primary specificity of five malarial enzymes, utilizing UV spectroscopic techniques, and the extended subsite binding preferences, determined using liquid chromatography−electrospray mass spectrometry (LC−MS)[1] analysis of substrate cleavage products.

The crystal structure of *P. falciparum* plasmepsin 2 (PfPM2) has revealed that the uncomplexed active-site cavity adopts an open conformation and has significant flexibility to accept bulky groups into its active site, whereas in the structure of the PfPM2−pepstatinA complex, this cavity is closed and tightly interacting with the inhibitor (*18*, *19*). Hence, because of this ambiguity in the structural conformation of this very mobile PfPM2 active site, there is insufficient structural information on the possible conformational modes of action of the various classes of competitive inhibitors to the PfPM2 or plasmepsins in general. Therefore, to provide an initial, although limited, structural context for interpreting our observed K_i values, computational-modeling methods were performed to examine the possible modes of binding for the peptidomimetic inhibitors. The protein templates used for these studies were all based on the coordinates of PfPM2 bound with the inhibitor rs370 (*20*); the rationale for this choice is that this is the highest resolution (1.8 Å) crystal structure of PfPM2, the binding cavity in the PfPM2−rs370 complex more closely represents the conformation of enzyme when natural substrate hemoglobin is bound, and the PfPM2 structure is in a relatively relaxed conformation and more appropriate for docking studies than it is in the pepstatin A complex.

EXPERIMENTAL PROCEDURES

All reagents for protein production and purification were purchased from Fisher Scientific unless otherwise noted. Competent cells were purchased from Novagen or Invitrogen. Anion-exchange chromatography was performed on a Pharmacia Biotech FPLC using a 5 mL HiTrap Q Sepharose High-Performance anion-exchange column purchased from Amersham Biosciences. Gel-filtration chromatography was performed using a BioRad 1.0 × 100 cm column equipped with a flow adapter and packed with Superdex 75 prep-grade gel-filtration resin from Amersham Biosciences. The SDS−PAGE reagents and equipment were purchased from BioRad. Peptide synthesis and purification were performed by the Protein Chemistry Core Facility at the University of Florida, Gainesville, FL. Resins and amino acids used to synthesize peptides and inhibitors were purchased from Nova Biochem. All peptide libraries were examined by amino acid analysis, high-pressure liquid chromatography (HPLC) separation, and mass spectrometry to verify the expected amino acid composition. LC−MS analysis was performed by Spectroscopy Services in the Chemistry Department at the University of Florida, Gainesville, FL.

Genes encoding the zymogens of PfPM2, PmPM4, PoPM4, and PvPM4 were cloned from genomic DNA by PCR amplification (*12*, *21*, *22*). PfPM4 was amplified from genomic DNA and cloned into a pCR2.1 vector (Invitrogen). Subsequently, the gene-coding region was digested from this vector using *Bam*HI (New England Biolabs) and was subcloned into the pET3a expression vector (Novagen). The pET3a plasmid containing the PfPM4 gene was transformed into BL21 (DE3) pLysS *Escherichia coli* cells (Invitrogen) for expression (*12*). All plasmepsin enzymes were expressed in *E. coli* and purified in inclusion-body form using the methods previously described (*23*). The inclusion bodies were isolated, solubilized, refolded, and purified using published protocols (*21*). Short recombinant human cathepsin D (hCatD) used in inhibition assays was expressed as previously described (*24*), refolded, and purified according to a modified protocol (*25*). The concentrations of catalytically active enzymes were determined by active-site titration assays with a single octapeptide substrate (KPIEF*NphRL) and a tight binding inhibitor (pepstatin A) (*25*).

Chromogenic peptide substrates and reduced peptide inhibitors were prepared by solid-phase synthesis using an Applied Biosystems 432A or 430A automatic peptide synthesizer (ABI, Foster City, CA) by either the 2-(1H-benzotriazole-1-yl)-1,1,3,3-tetramethyluronium hexafluorophoshate (HBTu)/*N*-hydroxybenzotriazole (HOBt) or *N*,*N*′-dicyclohexylcarbodiimide (DCC)/HOBt method. All single peptides were determined to be >95% pure by HPLC using a Beckman Coulter 127NMP system equipped with a reverse-phase C18 column from Vydac. The MALDI−TOF MS analysis of peptides was performed on a Voyager DE Pro BioSpectrometry WorkStation from Perseptive Biosystems

[1] Abbreviations: PfPM2, *Plasmodium falciparum* plasmepsin 2; PfPM4, *Plasmodium falciparum* plasmepsin 4; PoPM4, *Plasmodium ovale* plasmepsin 4; PmPM4, *Plasmodium malariae* plasmepsin 4; PvPM4, *Plasmodium vivax* plasmepsin 4; hCatD, human cathepsin D; TFA, trifluoroacetic acid; DTT, dithiothreitol; TIS, triisopropylsilane; Pbf, 2,2,4,6,7-pentamethyldihydrobenzofuran-5-sulfonyl; DCC, *N*,*N*′-dicyclohexylcarbodiimide; HOBt, *N*-hydroxybenzotriazole; Boc, *tert*-butoxycarbonyl; tBu, *tert*-butyl; HBTu, 2-(1H-benzotriazole-1-yl)-1,1,3,3-tetramethyluronium hexafluorophoshate; Fmoc, 9-fluoroenylmethoxycarbonyl; Trt, triphenylmethyl; Nph, *para*-nitrophenylalanine; Nle or nL, norleucine; Xaa, 19 amino acid mixture; LC−MS, liquid chromatography/electrospray mass spectrometry.

using α-cyano-4-hydroxycinnamic acid as the matrix. Concentrations of dissolved peptides were determined by amino acid analysis using an Applied Biosystems 420H Derivatizer.

P1 Library. For the combinatorial library approach, 19 pools of the following sequence were synthesized: Lys-Pro-(Xaa)-Glu-P1*Nph-(Xaa)-Leu, where the asterisk indicates the expected point of cleavage. In this library, the P1 represents a fixed amino acid (the 20 common amino acids except for Cys and Met, plus norleucine [Nle or nL]) for each pool. (Xaa) indicates that a mixture of the same 19 amino acids was incorporated at that given position. Peptides libraries were synthesized using Applied Biosystems (ABI) automatic peptide synthesizers (ABI 430A and 432A) with either the DCC/HOBt or the HBTu/HOBt methods. Peptides were assembled with the 9-fluoroenylmethoxycarbonyl (Fmoc)/*tert*-butyl (tBu) strategy using L-leucine 2-chlorotrityl resin (Nova Biochem). Fmoc amino acids [Fmoc-Ala, Fmoc-Arg-[2,2,4,6,7-pentamethyldihydrobenzofuran-5-sulfonyl (Pbf)], Fmoc-Asn[triphenylmethyl (Trt)], Fmoc-Asp(*O*-tBu), Fmoc-Gln(Trt), Fmoc-Glu(*O*-tBu), Fmoc-Gly, Fmoc-His(Trt), Fmoc-Ile, Fmoc-Leu, Fmoc-Lys[*tert*-butoxycarbonyl (Boc)], Fmoc-Nle, Fmoc-Phe, Fmoc-Pro, Fmoc-Ser(tBu), Fmoc-Thr(tBu), Fmoc-Trp(Boc), Fmoc-Tyr(tBu), and Fmoc-Val] were mixed in a molar ratio according to Backes et al. (*16*). The first two coupling reactions were 6-fold in excess DCC/HOBt on an ABI 430A, with the remaining coupling reactions 3-fold in excess HBTu/HOBt on an ABI 432A. The peptides were cleaved from the resin using a modified King's cocktail [trifluoroacetic acid (TFA), 87%; water, 5%; thioanisole, 5%; dithiothreitol (DTT), 2.5%; triisopropylsilane (TIS), 0.5%] for $1^1/_2$ h at room temperature. The resin was removed by filtration, and the resulting peptides were concentrated with nitrogen, washed several times with cold tBu methyl ether, dissolved in dilute acetic acid, and lyophilized.

P1′ Library. The P1′ combinatorial library was based on the same general sequence as the P1 library; however, the optimal residues determined from the P1 library analyses with the plasmepsins were incorporated at the P3 and P2′ positions and a Nph chromophore was incorporated at the P1 position. As a result, the P1′ library was comprised of the amino acid sequence Lys-Pro-Ile-Xaa-Nph*P1′-Gln-Xaa. For this library, peptides were synthesized in a manner similar to the P1 library, with the following exceptions. Peptides were assembled with the Fmoc/tBu strategy using a mixture of L-Xaa 2-chlorotrityl resins, such that Xaa was the mixture of the 19 different amino acids to be incorporated at the P3′ position. In this synthesis, the Fmoc amino acid molar ratios were adjusted to optimize coupling at the P2 position using relative abundances obtained from LC−MS for the octapeptide Lys-Pro-Ile-Xaa-Nph*Phe-Arg-Leu. The mole percents of the amino acids used to synthesize the P1′ library were as follows: [(amino acid, mole percent) Fmoc-Ala, 4.5; Fmoc-Arg(Pbf), 4.1; Fmoc-Asn(Trt), 4.4; Fmoc-Asp(*O*-tBu), 4.1; Fmoc-Gln(Trt), 5.2; Fmoc-Glu(*O*-tBu), 5.5; Fmoc-Gly, 6.0; Fmoc-His(Trt), 4.3; Fmoc-Ile, 17; Fmoc-Leu, 4.3; Fmoc-Lys(Boc), 4.3; Fmoc-Nle, 4.1; Fmoc-Phe, 3.7; Fmoc-Pro, 4.4; Fmoc-Ser(tBu), 6.0; Fmoc-Thr(tBu), 4.3; Fmoc-Trp(Boc), 4.2; Fmoc-Tyr(tBu), 4.4; and Fmoc-Val, 5.3].

Single Peptides. Peptidomimetic inhibitors incorporated a modified peptide backbone between the P1 and P1′ residues of the sequence, such that a reduced peptide bond or methyleneamino group (-CH_2-NH-) replaced the standard peptide bond (*26*). Peptides containing reduced peptide bonds were unable to be hydrolyzed by aspartic peptidases and can be used *in vitro* as competitive inhibitors (*27*).

Single penta- and tripeptides were synthesized to determine the HPLC elution order of isomeric peptides with identical molecular masses (when Xaa is Ile, Leu, and Nle) or with similar masses (when Xaa is Gln or Lys). Although high-energy MS/MS analysis results in distinguishable fragmentation of the side chains of isomeric amino acids (*28*, *29*), the low-energy instrument used in these assays was unable to perform this fragmentation. Therefore, the identification of isomeric peptides in our mixtures by this approach was not possible. The isomeric peptide sequences were assembled, and their retention times were deduced by LC experiments. Unknown isomeric peptides in the digested library pools were identified by correlating their retention times to the elution profiles of the control peptides.

Combinatorial Spectroscopic Assays. Spectroscopic assays measuring the initial velocities of cleavage for each pool of the P1 and P1′ combinatorial libraries were used to determine the primary subsite (S1 and S1′) preferences of the human and malarial peptidases. The lyophilized pools of the peptide libraries were resuspended at 1.25 mg/mL in sterile filtered ddH_2O and centrifuged on a 0.45 μm Costar cellulose acetate centrifuge tube filter at 20000*g* for 5 min to remove particulates. For a 250 μL final reaction volume, 20 μL of the stock solutions (ca. 1.25 mM) was used in the spectroscopic kinetic assays and the enzymatic digestions for LC−MS. Thus, the library pools were at ca. 100 μM final concentration in each assay. The final concentration of enzyme in the reaction ranged from 5 to 100 nM depending upon the activity of the individual plasmepsin preparations. The pH and ionic strength used in the assay have been experimentally determined to be the optimal conditions for maximal enzyme activity (*30*−*32*). For all plasmepsins, a preincubation for 5 min at 37 °C in 0.1 M sodium formate buffer at pH 4.5 was used to convert the zymogens to the mature enzymes before the addition of substrate (*21*, *31*, *33*). hCatD used in the inhibition assays was incubated at 37 °C in 0.2 M sodium formate buffer at pH 3.7 to equilibrate the mature enzyme to the assay temperature at which it was most active.

The initial velocities of enzyme-catalyzed cleavage of the P1 library (Lys-Pro-Xaa-Glu-P1*Nph-Xaa-Leu) and the P1′ library (Lys-Pro-Ile-Xaa-Nph*P1′-Gln-Xaa) were observed on a Hewlett−Packard 8452A Diode Array spectrophotometer equipped with a multicell transport and a thermostated circulating water bath set to yield 37 °C in the cuvettes (*33*). The scissile peptide bond indicated by the asterisk shows the point of enzymatic cleavage, which results in a decrease or increase in the average UV absorbance from 284 to 324 nm of the Nph for the P1 or P1′ libraries, respectively (*33*). The collection of rate data was measured over 3600 s to observe the total cleavage of the library pools. However, only the linear phase of the substrate-cleavage reactions was used to determine the primary specificity preferences. The resulting initial velocities of cleavage for each library pool were normalized with the maximal rate set to 100 percent; therefore, the preferences of the different peptidases could be easily compared.

Analyses of Cleavage Products. The P1 and P1′ library peptide pools showing the fastest cleavage by the UV rate assay were digested in the same way as in the initial velocity studies, but after 5 min of enzyme-catalyzed digestion, an aliquot of 1.5 M ammonium hydroxide was added to a final concentration of 90 mM to raise the pH of the reaction to greater than pH 8.0. At this increased pH, the plasmepsins were rendered inactive, thereby halting the hydrolysis of the octapeptide substrates under initial velocity conditions. These samples were subsequently analyzed by LC−MS to determine the relative abundances of the penta- (Lys-Pro-Xaa-Glu-Phe or Lys-Pro-Ile-Xaa-Nph) and tri- (Nph-Xaa-Leu or Phe-Gln-Xaa) peptide cleavage products.

HPLC Separation of Peptides. HPLC of product mixtures was accomplished with a Beckman (Beckman Instruments, Fullerton, CA) model 126 pump and the System Gold (version 7.11) software. A binary-gradient system consisted of mobile phase A being 0.5% glacial acetic acid in water and mobile phase B being 0.5% glacial acetic acid in methanol. The column used was a Waters (Waters Corp., Milford, MA) Symmetry RP18 column (2.1 mm inside diameter × 150 mm length, 3.5 μm particle size) with either an RP18 guard column or a Phenomenex (Torrance, CA) LUNA C18 guard column. Experiments with a LUNA C18 analytical column (2.1 × 150 mm) showed better retention of the more polar pentapeptides but poorer separation overall than did the Symmetry RP18 column. The LUNA guard−RP18 analytical column combination yielded a good compromise. The gradient typically used was as follows:

time (min)	0	0.1	40.1	75.1	76	86	106	107	108
A/B	100:0	100:0	60:40	35:65	35:65	100:0	100:0	100:0	100:0
mL/min	0.15	0.15	0.15	0.15	0.2	0.2	0.2	0.15	0.15

Mass Spectrometric Analyses of Peptides. All mass spectrometric data were acquired with a Thermo-Finnigan (San Jose, CA) LCQ "Classic" quadrupole ion trap mass spectrometer operated in the electrospray ionization (ESI) mode, typically with the following conditions: sheath gas (N_2), 60; aux gas (N_2), 5; spray voltage, 3.5 kV; capillary temperature, 240 °C; capillary voltage, 15 V; and tube lens offse, 0 V. The (+)ESI−normal mass spectra were acquired over the expected *m*/*z* range (e.g., *m*/*z* 230−800) of the $[M + 2H]^{2+}$, $[M + H]^+$, and $[M + Na]^+$ ions of the pentapeptides and the $[M + H]^+$ ions of the tripeptides with the automatic gain control (AGC) set to 200 million counts, with either 2 or 3 microscans. The tripeptides yielded few or no detectable $[M + 2H]^{2+}$ ions. Tandem mass spectrometry (MS/MS) daughter spectra of nonisomeric overlapping peptides were obtained with a parent ion isolation of 3−5 amu and a percent CID energy of 35−40%, either under manual control or with the dependent MS/MS function under LCQ software control.

Peak-Area Integration. After the analysis, the pertinent peak areas were integrated utilizing mass chromatograms of the characteristic ions that resulted from HPLC separation of the peptide mixtures, which yielded the abundance of each peptide present in the mixture. For most of the pentapeptides, the $[M + 2H]^{2+}$ and $[M + H]^+$ ions yielded significant peaks. For several of the pentapeptides, which eluted just after the void volume, there were significant levels of the $[(M - xH + xNa) + Na]^+$ ions, where *x* protons had been replaced by *x* Na^+ ions, where $x = 0, 1, 2$, etc., in addition to the protonated molecules.

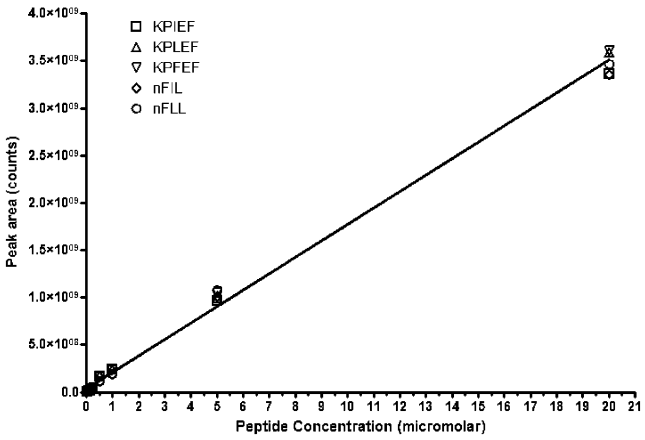

FIGURE 1: Calibration curve to determine the extent of pentapeptide and tripeptide ionization in LC−MS analyses. (□) KPIEF, (△) KPLEF, (▽) KPFEF, (◇) nFIL, and (○) nFLL.

The integration of mass peaks produced from LC−ESI is semiquantitative, because peptides of various size and amino acid composition ionize differently. The ability of our peptides to ionize was tested with a sample set of peptides, for which the concentration of each substituent was determined by amino acid analysis prior to the preparation of the stock solution. The stock solution was prepared as described for the combinatorial libraries, and serial dilutions (50 nM−20 μM penta- and tripeptides) were performed with sterile filtered water. The concentrations of peptides used to determine the calibration curve cover the range of the majority of all ion peaks, which generally fell between 1 million and 2 billion counts. From this assay, equivalent amounts of each sample peptide were observed with the electrospray technique over the concentration range in which the majority of the cleavage products were observed, suggesting that peptides in this mass range ionize with relatively equal intensity (Figure 1).

Normalizations of the initial velocity and relative abundance data were performed by taking the highest value for the kinetic or peak areas, respectively, and scaling it to a value of 100. All remaining data for a given enzyme with a peptide library pool were reported as a percentage of the maximal value.

Design of Peptidomimetic Inhibitors. For each plasmepsin, the amino acid residues preferred were compared to the results obtained for hCatD (data not shown) with the P1 and P1′ libraries. The substitutions that conferred the largest amount of specificity for the malarial enzymes versus hCatD were incorporated into synthetic methyleneamino [-CH_2-NH-] inhibitors, which were used to determine inhibition constants.

Inhibition Studies. All kinetic data were fitted using the Enzyme Kinetic Module (version 1.0) of SigmaPlot 2000 (version 6.10) to determine inhibition constants.

The dissociation constant (K_i) was obtained by observing the decrease in substrate hydrolysis with the inhibitor present, which resulted in an apparent increase in the K_m value. The V_{max} and K_m values were determined as previously described with at least six substrate concentrations in the absence of the inhibitor. After this curve was obtained, at least two

additional curves were plotted using the initial rates of cleavage of six substrate concentrations in the presence of the inhibitor, with at least two inhibitor concentrations used. After a Michaelis−Menten curve was obtained, the K_i was then determined by simultaneously fitting all of the data to the following equation:

$$v = ([S]V_{max})/([S] + (K_m(1 + [I]/K_i))) \quad (1)$$

The inhibition constant for tight binding inhibitors was determined with the competitive tight binding inhibitor equation, such that $K_i^{ap} = (K_i([S]/K_m + 1))$ (*34*)

$$v = \{(2[E]V_{max})/(K_m/[S] + 1)\}\{([E] - [I] - K_i^{ap}) + \sqrt{(([E] - [I] - K_i^{ap})^2 + (4[E]K_i^{ap}))}\} \quad (2)$$

Computational Studies. Three-dimensional models of PfPM4, PvPM4, PoPM4, PmPM4, and hCatD were all built based on the template of the PfPM2 coordinates (PDB ref 1lf2) obtained from the crystal structure of the PfPM2−rs370 complex (*20*). Models were built using SWISS-MODELLER (*35*, *36*) and internally evaluated with the automatic tool WHATIF-Check. The peptidomimetic inhibitors were modeled using the molecular-modeling program SYBYL (version 6.9, Tripos Inc.) (*37*). The 3D conformations of inhibitors were built using the Composer routine in the Biopolymer module of SYBYL. Energy minimizations of the inhibitors were carried out using the standard Tripos force field, and a conjugated gradient convergence method was used with termination criterion of the gradient set at 0.05 kcal/mol energy.

Docking calculations were performed using Autodock version 3.0 (*38*). The crystallographic coordinates of the inhibitor rs370 were used as the reference to manually adjust and approximate the position of peptidomimetic inhibitors. The maps were centered on the center of gravity of the ligand-binding site and were calculated using AutoGrid. For all of the docking calculations, a grid map with $78 \times 112 \times 92$ points and grid-point spacing of 0.25 Å (roughly $^1/_5$ of the length of a carbon−carbon single bond) were used.

Docking runs were performed using the Lamarckian Genetic Algorithm as discussed previously (*38*−*40*). For all dockings, 10 independent runs with step sizes of 2 Å for translations and 5° for orientations and torsions were performed. An initial population of random individuals with a population size of 100 individuals, a maximum number of 2×10^6 energy evaluations, a maximum number of generations of 50 000, an elitism value of 1, a mutation rate of 0.02, and a crossover rate of 0.8 were used. The pseudo-Solis and Wets local search methods were used with default parameters. The number of iterations per local search was 300. The possibility of performing a local search on an individual in the population was 0.06. The maximum number of consecutive successes or failures before doubling or halving the local search step size was 4, and the termination criterion for the local search was 0.01. The clustering tolerance for the root-mean-square positional deviation was 0.5 Å. The conformation with the lowest energy was used for the analysis of binding the inhibitor with the enzyme.

The K_i values were obtained from the computationally calculated estimated free energy of binding (ΔG) using the equation $K_i = \exp(\Delta G/RT)$, where R (ideal gas constant) is 1.987 cal K^{-1} mol^{-1} and T (temperature) is 298.15 K.

RESULTS

Synthesis. The amounts of amino acids for solid-phase peptide synthesis were based on Backes et al. (*16*); however, our analyses revealed that this ratio was not optimal in our library syntheses to obtain equimolar concentrations at the position of the mixture. To observe the extent of amino acid coupling, octapeptides of the sequence KPIEFNphXL, KPIXFNphQL, and KPIEFNphQX were synthesized. Each synthesis would result in a pool containing 19 different octapeptides. LC−MS separation and analysis was performed on these pools to determine the abundance of each of the 19 octapeptides. The resulting peak areas were used to adjust for the differences in the coupling of various amino acids during peptide synthesis.

Subsite Preferences, S1 and S1′. To qualitatively analyze the preference of each library pool, a ranking system was devised with the following scheme. Amino acids observed in the range of 67−100% of the normalized initial velocities were considered good or readily acceptable substitutions, whereas peptides from 0 to 33% of the normalized initial velocities were considered poor substitutions. Substitutions falling between these two regions, i.e., 34−66%, were of average or moderate acceptance. This ranking system will also be employed to qualitatively examine the results obtained for extended specificity preferences using LC−MS analyses.

The initial velocities of each reaction were determined from the slope of the linear phase and were plotted for each P1 (Figure 2) or P1′ (Figure 3) substitution for the malarial enzymes. The values for each enzyme were normalized and plotted together to observe the differences in the P1 or P1′ specificities. The P1 substitutions phenylalanine, leucine, and Nle provided rapid rates of cleavage and, thus, were readily acceptable P1 residues, which is consistent with other observations in the literature for various members of the aspartic peptidase family (*41*−*43*). The most noticeable difference in P1 specificity was observed with PfPM2, which prefers Nle as the best substitution. All other plasmepsins accept phenylalanine as the ideal substitution at this subsite. The other plasmepsin analyzed from *P. falciparum* (PfPM4) also had a unique S1 specificity preference. While phenylalanine is the optimal P1 substitution, it is also the only amino acid of average acceptance or better. The rates of cleavage for the P1 library by PfPM4 reveal that leucine and Nle were poorly accepted, because they were 30 and 20% of the phenylalanine rate, respectively. The markedly different preferences observed for PfPM2 and PfPM4 suggest that these enzymes may cleave different sites in the globin chains of hemoglobin. Although phenylalanine, Nle, and leucine were the three best substitutions at the P1 position for PoPM4, leucine was only a poorly tolerated substituent. The PmPM4 and PvPM4 enzymes found Phe, Leu, and Nle as average or above average P1 residues; however, PmPM4 accepts phenylalanine and leucine almost equally. Another common trait between the plasmepsins is the intolerance of nonhydrophobic substitutions in the S1 subsite. Plasmepsin 2 shows a slight acceptance of tyrosine and alanine, but these amino acids remain poor substitutions. Also, a low ac-

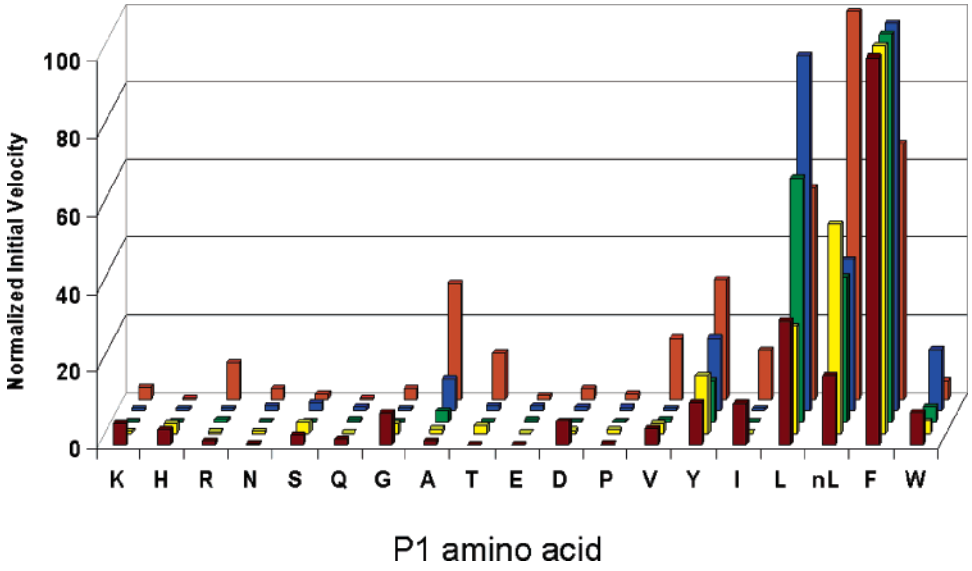

FIGURE 2: Bar graph of the normalized initial velocities for cleavage of the pools of the P1 library for PfPM2, PfPM4, PmPM4, PoPM4, and PvPM4. The P1 substitution of the library pool is indicated on the *x* axis. The activity assays were measured at 37 °C and 0.1 M sodium formate at pH 4.5. Burgundy, PfPM4; yellow, PoPM4; green, PvPM4; blue, PmPM4; and orange, PfPM2.

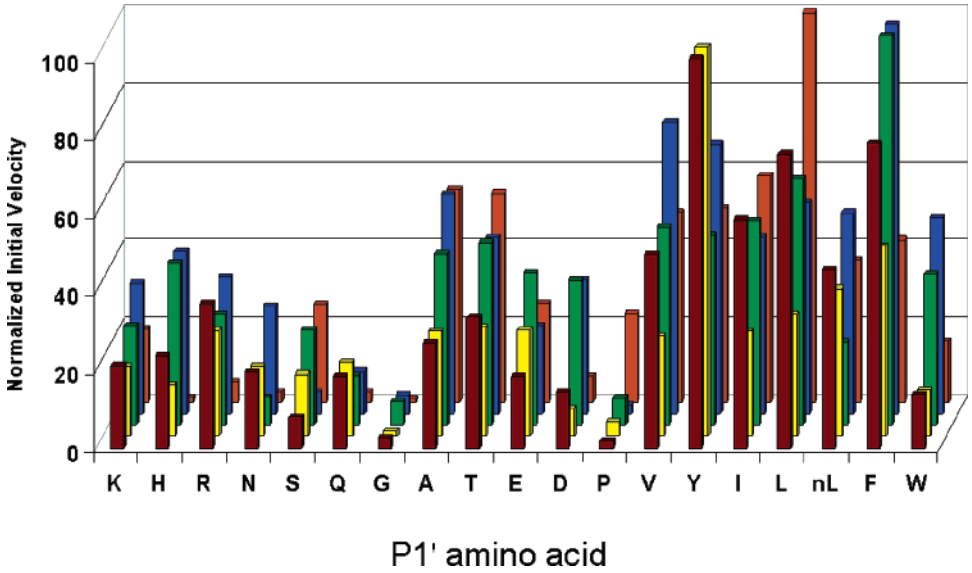

FIGURE 3: Bar graph of the normalized initial velocities for cleavage of the pools of the P1′ library for PfPM2, PfPM4, PmPM4, PoPM4, and PvPM4. The P1′ substitution of the library pool is indicated on the *x* axis. The activity assays were measured at 37 °C and 0.1 M sodium formate at pH 4.5. Burgundy, PfPM4; yellow, PoPM4; green, PvPM4; blue, PmPM4; and orange, PfPM2.

ceptance of tryptophan was observed at the S1 pocket for all plasmepsins studied here.

The best residues for the S1′ subsites of the plasmepsins were consistently hydrophobic substitutions. The aromatic residue phenylalanine is optimal at P1′ for PvPM4 and PoPM4, and tyrosine is the best amino acid for PmPM4 and PfPM4. Plasmepsin 2 differs dramatically from the other four plasmepsins, with the only above average substitution at the S1′ pocket being leucine. As noted with the results for the S1 subsite, PfPM2 and PfPM4 each possess a distinct amino acid preference at the P1′ position of a peptide substrate. Large aromatic hydrophobic substitutions, with the exception of Trp, were ideal for plasmepsin 4, but plasmepsin 2 prefers branched substitutions. Inspection of these preferences suggests PfPM2 had a smaller S1′ pocket, especially because alanine is the third best substitution at the P1′ position. Alanine was also found to be of average acceptance for PvPM4 and PmPM4.

Subsite Preferences, S3, S2, S2′, and S3′. LC−MS analyses of the pentapeptides formed from the hydrolysis of the P1-Phe pool revealed hydrophobic amino acid preferences at the S3 subsite of the plasmepsins, which were displayed in Figure 4. Similar to the observances for plasmepsin 2 at the S1 primary subsite, the S3 pocket of PfPM2 had a unique preference for Nle. The Nle substitution is tolerated by other enzymes but with slightly less intensity when compared to PfPM2. Plasmepsin 2 also accepts phenylalanine with equal felicity when compared to the other plasmepsins. Tryptophan is an average or above average substitution for all plasmepsins, but PoPM4 does not find it as favorable as the other four enzymes. Nonhydrophobic substitutions in P3 were generally poor for the plasmepsins, but this is especially the

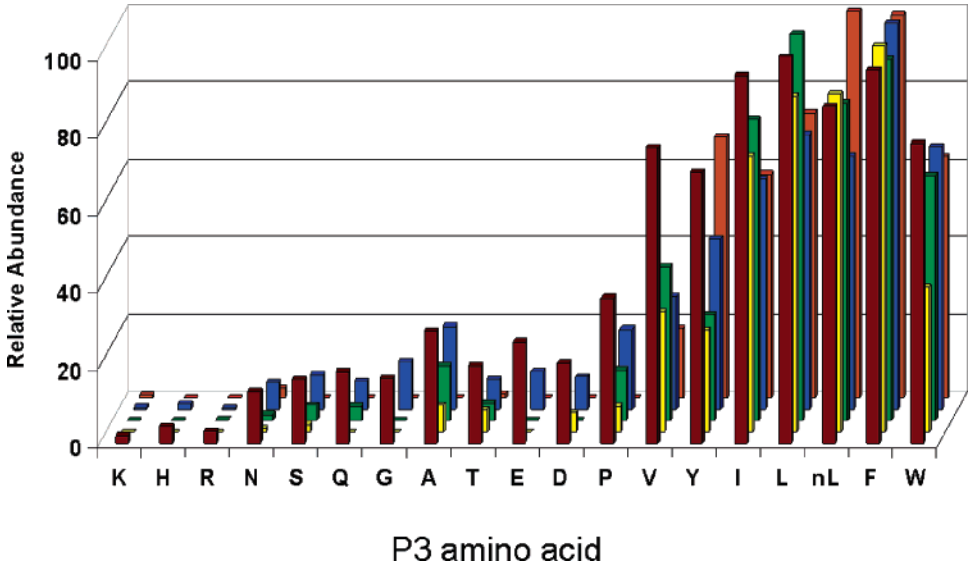

FIGURE 4: Bar graph of the normalized relative abundances for the pentapeptides produced by PfPM2, PfPM4, PmPM4, PoPM4, and PvPM4 catalyzed cleavage of the P1 phenylalanine containing pool of the P1 library. The P3 substitution of the library pool is indicated on the *x* axis. The activity assays were measured at 37 °C and 0.1 M sodium formate at pH 4.5. Burgundy, PfPM4; yellow, PoPM4; green, PvPM4; blue, PmPM4; and orange, PfPM2.

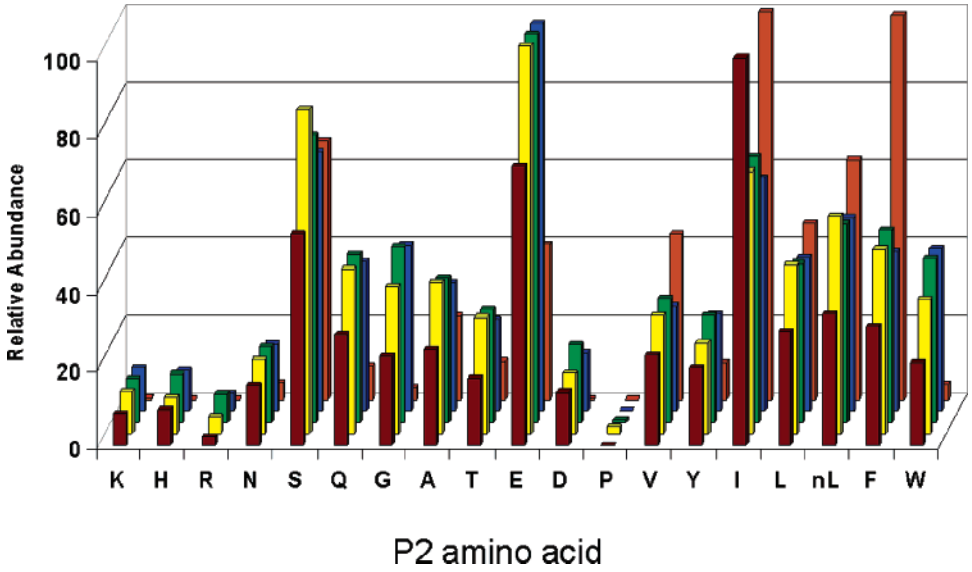

FIGURE 5: Bar graph of the normalized relative abundances for the pentapeptides produced by PfPM2, PfPM4, PmPM4, PoPM4, and PvPM4 catalyzed cleavage of the P1′ phenylalanine containing pool of the P1′ library. The P2 substitution of the library pool is indicated on the *x* axis. The activity assays were measured at 37 °C and 0.1 M sodium formate at pH 4.5. Burgundy, PfPM4; yellow, PoPM4; green, PvPM4; blue, PmPM4; and orange, PfPM2.

case for plasmepsin 2. From the subset of aspartic peptidases that have been screened in this study, it can be concluded that the S3 subsite is extremely hydrophobic, yielding a conserved specificity preference among malarial members of the A1 family of peptidases.

The relative abundances of the pentapeptides created from cleavage of the P1′-Phe pool were used to determine the specificity of the plasmepsins at the S2 subsite. The *P. falciparum* peptidases share a preference for isoleucine at the S2 pocket, yet plasmepsin 2 accepts phenylalanine almost as well as isoleucine (Figure 5). The three non-*P. falciparum* plasmepsins from the remaining species showed a large preference for peptides containing a P2 glutamic acid. Overall, hydrophobic substitutions were of average acceptance, while peptides containing a P2 serine or glutamate were preferentially cleaved by most enzymes. A poor acceptance of basic residues and proline at the P2 position was also observed with all malarial aspartic peptidases.

The relative abundances of the tripeptides formed from the hydrolysis of the P1-phenylalanine containing pool of the P1 library revealed the S2′ subsite specificity, which is detailed in Figure 6. The S2′ subsite had a much broader specificity than the other subsite pockets that were examined by the combinatorial method. Hydrophobic substitutions, especially Ile, were the best substitutions for PvPM4 and PmPM4, while PmPM4 strongly accepted tryptophan. There is an increased acceptance of basic residues at this position for the plasmepsins; however, plasmepsins 2 and 4 both share glutamine as the best P2′ substitution.

The tripeptides formed from plasmepsin-catalyzed hydrolysis of the phenylalanine-containing pool of the P1′ library revealed the amino acid preferences at the S3′ subsite

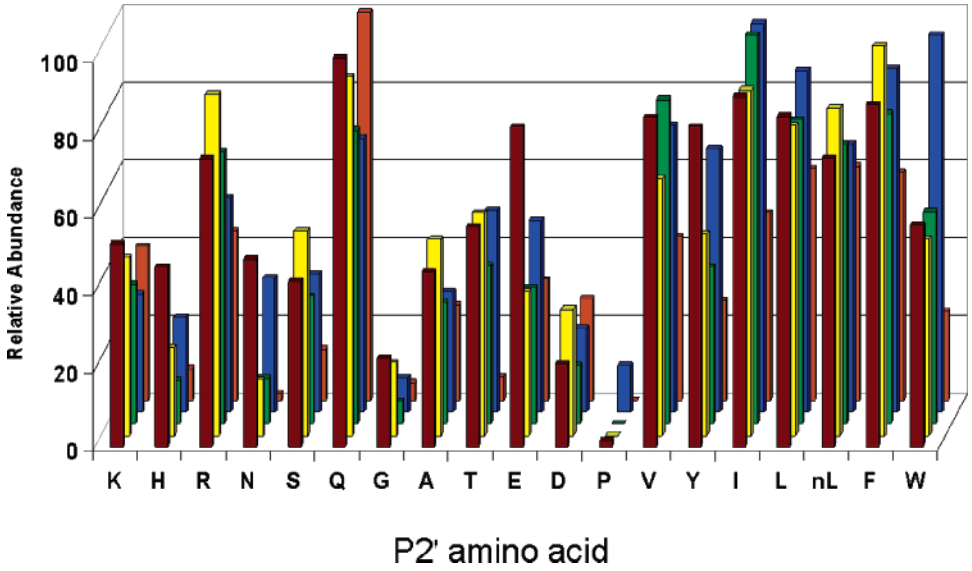

FIGURE 6: Bar graph of the normalized relative abundances for the tripeptides produced by PfPM2, PfPM4, PmPM4, PoPM4, and PvPM4 catalyzed cleavage of the P1 phenylalanine containing pool of the P1 library. The P2′ substitution of the library pool is indicated on the *x* axis. The activity assays were measured at 37 °C and 0.1 M sodium formate at pH 4.5. Burgundy, PfPM4; yellow, PoPM4; green, PvPM4; blue, PmPM4; and orange, PfPM2.

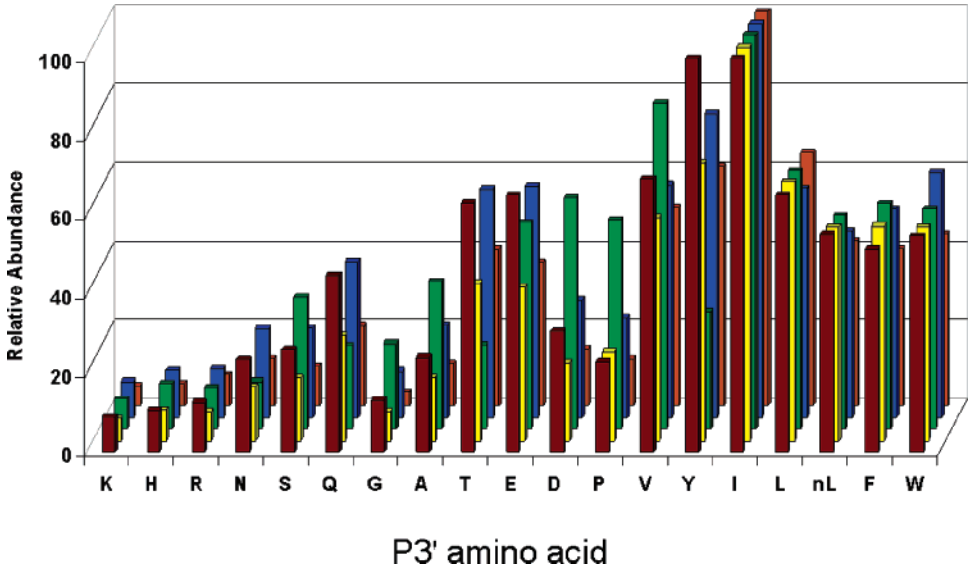

FIGURE 7: Bar graph of the normalized relative abundances for the tripeptides produced by PfPM2, PfPM4, PmPM4, PoPM4, and PvPM4 catalyzed cleavage of the P1′ phenylalanine containing pool of the P1′ library. The P3′ substitution of the library pool is indicated on the *x* axis. The activity assays were measured at 37 °C and 0.1 M sodium formate at pH 4.5. Burgundy, PfPM4; yellow, PoPM4; green, PvPM4; blue, PmPM4; and orange, PfPM2.

(Figure 7). The acceptances by the plasmepsins were broad at the P3′ position, as noted by the increased acceptances for small aliphatic, amide-containing, and acidic residues. Isoleucine was the preferred substitution of the plasmepsins, followed by tyrosine for PfPM4 and PmPM4 or valine for PvPM4. The remaining hydrophobic amino acids were moderately accepted for all plasmepsins. Isoleucine was far better than any other substitution for PfPM2 and PoPM4, because it was approximately 30% better than the nearest substitutions of leucine or tyrosine, respectively.

Threonine and glutamate were two of the average substitutions for PmPM4 and PfPM4 with abundances equal to $^1/_2$ of the value of the best substitution. Similar relative abundances were observed for aspartate and proline with PvPM4.

These data encompass the S3−S3′ sites of the binding cleft, including the pockets that confer primary preferences. Additionally, a larger set of residues were screened at each position in comparison to previous methods (*12*, *21*, *31*), which increases the probability of designing a sequence that specifically and tightly binds the plasmepsins. However, in this study, we have relied on the common amino acids found in proteins and have not included nonnatural amino acids other than Nle.

Inhibitor Design and Analysis. The design of a series of inhibitors was completed using the specificity information obtained from analysis with the P1- and P1′-combinatorial peptide libraries. The design of this series of peptidomimetic compounds incorporated the amino acid residue at each position that had the highest relative abundance or normalized

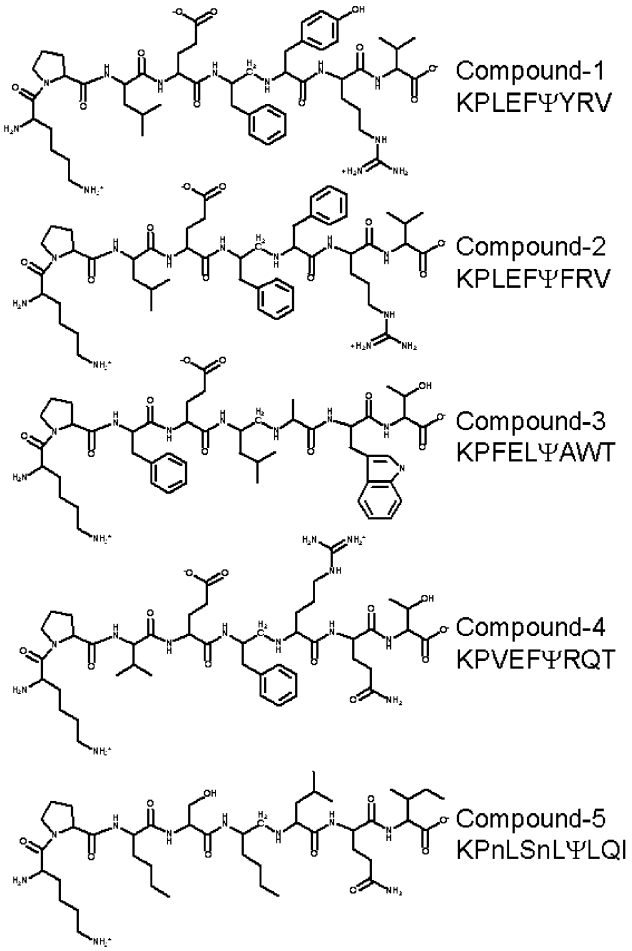

FIGURE 8: Structures of the five methyleneamino-reduced peptide inhibitors designed from the results of the combinatorial approach.

initial velocity in comparison to a human homologue, hCatD (data not shown). This strategy would hopefully result in the identification of potent and selective inhibitors of the plasmepsin that would not interact with hCatD.

The structures of the five inhibitors designed from the results of the combinatorial approach are detailed in Figure 8. Although the majority of these inhibitors retain hydrophobic characteristics at the primary binding positions, two of the compounds (compounds 3 and 4) incorporate an aliphatic or a basic residue at the P1′ position, respectively. Kinetic analyses with these inhibitors yielded inhibition constants that spanned orders of magnitude (Table 1), such that compound 3 was poorly accepted (>10 μM) by all of the aspartic peptidases.

The only inhibitors in this series to give picomolar inhibitory constants were compounds 1 and 2. These two inhibitors share the same sequence except for the P1′ residue, where the P1′ phenylalanine of compound 1 is replaced by a tyrosine in peptidomimetic compound 2. These two compounds were not tolerated by PfPM2, which resulted in micromolar values with peptidomimetic compounds 1 and 2 (19.5 and 4.32 μM, respectively). In contrast, compound 2 resulted in an inhibition constant of 85 pM against PfPM4, which is 55-fold lower than the 4.7 nM value observed for hCatD.

The peptidomimetic compounds designed against the *P. falciparum* enzymes (PfPM4, compound 4; and PfPM2, compound 5) were observed to be nanomolar inhibitors for all enzymes, except for compound 4 with PfPM2. The value for this inhibition constant was not obtained, because a final concentration of 20 μM of compound 4 did not decrease the initial velocities of PfPM2-catalyzed substrate hydrolysis. However, compound 4 inhibited the enzyme to which it was targeted (PfPM4) with a K_i of 2.4 nM, which is almost 13-fold better than the value observed for hCatD. Compound 5 tightly bound all of the plasmepsins, and these K_i values were all lower than the inhibitory constant for hCatD. Plasmepsin 2 resulted in the tightest binding (13.9 nM) of peptidomimetic compound 5, which was over 15-fold better than hCatD with this inhibitor. Plasmepsin 4 had the second best K_i with compound 5, which was 21.7 nM.

The only peptidomimetic sequence that was unsuccessful against any of the aspartic peptidases was compound 3. All values obtained with this inhibitor ranged from 9.0 to greater than 20 μM. However, it is notable that the lowest K_i of 9.0 μM was observed with PmPM4, which was the target enzyme of this compound. The poor inhibitory effects can possibly be attributed to the incorporation of an alanine at the P1′ position, which was found to be accepted almost half as well as the best P1′ substitution of phenylalanine (Figure 3). The deleterious effects on the binding constants reveal the importance of the enzyme−ligand interactions at the primary specificity pockets. Compounds 1 and 2 were tested against *P. falciparum* in culture and exhibited apparent IC_{50} values of 52 and 58 μM, respectively (Fiddock, D. and Dame, J. B., unpublished results). Other compounds related to 1−5 exhibited similar IC_{50} values; thus, it might be concluded that it is difficult for these basic compounds to enter cells.

Computational Studies. To assess the mode of inhibitory action of the compounds further, compounds 1−5 were computationally evaluated for their K_i values against all five plasmepsins and the human homologue hCatD. The calculated K_i values and active-site interactions from the molecular-modeling studies of the five compounds to the five plasmepsins (PfPM2, PfPM4, PvPM4, PoPM4, and PmPM4) and the human homologue hCatD are given in Table 2.

Overall, the mean inhibition constant for compounds 1, 2, 4, and 5 were ranked as pico- to nanomolar, whereas compound 3 was at best a micromolar inhibitor (Table 2). The experimentally measured K_i results were fairly consistent

Table 1: Inhibition Constants for Five Methyleneamino-Reduced Peptide Inhibitors with Malarial Plasmepsins and hCatD

peptidase	compound 1 (nM)	compound 2 (nM)	compound 3 (nM)	compound 4 (nM)	compound 5 (nM)
PoPM	3.2 ± 0.5	3.2 ± 0.5	>20 000	39.0 ± 4.5	187 ± 29
PvPM	0.68 ± 0.09	0.58 ± 0.08	9800 ± 1800	14.4 ± 2.1	96.9 ± 14.0
PmPM	0.34 ± 0.05	3.7 ± 0.6	9000 ± 1200	10.3 ± 1.3	160 ± 26
PfPM4	0.48 ± 0.09	0.09 ± 0.02	12 700 ± 1600	2.37 ± 0.32	21.7 ± 2.7
PfPM2	19 500 ± 400	4320 ± 750	16 600 ± 3100	20 000	13.9 ± 1.8
hCatD	8.5 ± 0.6	4.7 ± 0.4	12 700 ± 1200	30.4 ± 2.0	219 ± 21

Table 2: Computational-Modeling Studies: Calculated K_i (in Nanomolars) and Number of Hydrogen Bonds (H-B) and Hydrophobic (HPhob) Interactions[a] for Compounds 1−5 for the Five Plasmepsins (PfPM2, PfPM4, PvPM4, PoPM4, and PmPM4) and the Human Homologue hCatD

compound		PfPM2	PfPM4	PvPM4	PoPM4	PmPM4	hCatD
1	K_i[b]	0.110	0.752	1.16	**2.98**	0.985	32.1
	H-B/HPhob	4:18	4:13	5:10	**9:10**	5:13	6:10
2	K_i[b]	266	5.38	**16.6**	0.711	5.90	80.6
	H-B/HPhob	1:14	6:11	**3:11**	3:14	6:10	4:14
3	K_i[b]	26.6	159	416	70.8	**10.3**	1610
	H-B/HPhob	3:14	5:13	0:12	7:8	**7:13**	3:10
4	K_i[b]	5.91	**5.09**	6.43	0.044	12.4	291
	H-B/HPhob	6:13	**5:12**	4:11	6:12	0:15	4:8
5	K_i[b]	**66.8**	6.18	166	1.96	20.5	1490
	H-B/HPhob	**5:10**	4:7	3:12	5:9	0:12	3:9

[a] The number of calculated [hydrogen bonds (H-B)/hydrophobic (HPhob)] interactions as defined by LIGPLOT (*49*). [b] The calculated K_i for these compounds has been adjusted [by 0.3113 kcal mol^{-1} (torsional degree of freedom)$^{-1}$] to account for differences in the number of torsional degrees of freedom for each compound (*38*). Bold indicates the plasmepsin that the compound was targeted against.

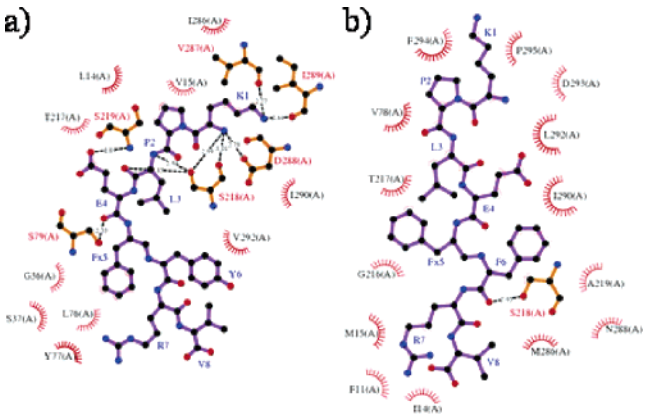

FIGURE 9: Schematic depiction of a modeled, experimentally measured "good" and "poor" plasmepsin inhibitor. (a) Compound 1 modeled into PoPM4. (b) Compound 2 modeled into PfPM2. The inhibitors are represented as ball-and-stick models (amino acid numbering in blue). The respective plasmepsin residues (amino acid numbering in black, identified by an "A" in parentheses) that exhibit hydrogen-bonding interactions (dashed lines) are represented as ball-and-stick models, while those exhibiting hydrophobic interactions with the inhibitor are represented by curved comb lines. Compound 1, which shows 9 hydrogen bonds and 10 hydrophobic interactions in the active site of PoPM4, has an experimentally determined low K_i (mostly likely because of a combination of numerous interactions). Compound 2 shows the presence of primarily hydrophobic interactions and has an experimentally determined high K_i (implying that good inhibitors require specific hydrogen-bonding interactions). Residue Fx5 in both inhibitors represent a modified phenylalanine with CH_2 instead of the C═O bond. This figure was made using LIGPLOT (*49*).

with the computational docking studies where compounds 1 and 2 had calculated K_i values in the picomolar range. The docking of compound 2 with PfPM2 showed a high K_i value of 0.266 μM, compared to the other calculated K_i values of the plasmepsins. This could be due to the lack of hydrogen-bonding interactions stabilizing the inhibitor in the binding pocket (Table 2 and Figure 9). Similarly to the experimental observations, compound 2 gave calculated K_i value of 5.38 nM (15-fold lower) and 0.711 nM (113-fold lower) against PfPM4 and PoPM4, respectively, than that observed for hCatD.

The computational modeling also showed that compounds 4 and 5 had nanomolar inhibitory constants for all enzymes (with the exception of compound 4 with PoPM4, which showed picomolar inhibition). The computational calculated K_i value for compound 4 against PfPM4, for which it was designed, was 5.09 nM, which is in close agreement with the experimental value of 2.4 nM. Similarly, for compound 5 designed against PfPM4, the computational value (66.8 nM) was in good agreement with the experimental measured value.

Finally, the computed K_i values for compound 3 against all plasmepsins were also very high relative to the K_i values of other compounds (Table 2) and therefore in agreement with the experimental data. The modeling studies implied that the alanine at the P1′ position had only very modest hydrophobic interactions with the plasmepsins, which could be the rationale for the higher K_i values. Interestingly, the modeling, which resulted in lower K_i values, was of compound 3 against PfPM2 and PmPM4, which possibly could be attributed to hydrogen-bonding interactions between the active-site residue (S218 in PfPM2 and G78 in PmPM4) and O (carbonyl) of alanine at the P1′ position (data not shown).

Also, the mean calculated K_i values for all compounds (~700 nM) were very high for hCatD (Table 2). In general the calculated K_i values were lower than those measured, but the overall trend in apparent inhibition was the same. These differences in measured and calculated K_i values may be attributed to both the experimental conditions as well as assumptions made in the molecular-modeling calculations.

DISCUSSION

An ideal drug targeted against *Plasmodium* would have specific activity against all species that infect humankind. Although plasmepsins from each of the four species have been cloned and expressed as recombinant enzymes (*12*, *18*, *22*, *44*, *45*), there is still very little known about many of the peptidases recently discovered from the *P. falciparum* genome-sequencing project (*46*). The most fully characterized plasmepsin is PfPM2, where numerous structures (*18*−*20*) and kinetic studies (*21*, *31*, *45*, *47*) have aided in identifying the determinants of substrate specificity.

The combinatorial method screened 6859 different peptides for each library in a relatively short period of time when compared to single peptide studies. The combinatorial library approach allows for a large number of peptides to be screened in one assay, and the library screening can quickly be expanded to more enzymes of the A1 family of peptidases to uncover specific interactions within an active site. As new *Plasmodium* plasmepsins are cloned, expressed, and purified, they can be subsequently analyzed with the peptide libraries and compared to current results.

The inhibition studies have verified that the targeted chromogenic combinatorial library approach is a viable method by which to screen the preferences of peptidases. The sequences of the compounds used in the inhibition analyses were generally tight-binding inhibitors of the plasmepsins. With four of the inhibitors, there was up to 55-fold selectivity to their target enzyme versus hCatD. Picomolar inhibitors were identified with the compounds for the orthologous plasmepsins, whereas low nanomolar inhibitors of plasmepsin 2 were observed from these studies.

The calculated K_i values from the molecular-modeling studies demonstrate a good correlation to the experimentally measured values. This observation especially holds true for the weaker inhibitions; for example, for all five compounds against hCatD and for compound 3 against all of the plasmepsins. This would indicate that these computational methods would be a useful guide to differentiate between poor and good inhibitors and help in the design of new inhibitors.

In general terms, the molecular modeling also indicated that the mode of binding of these peptidomimetic inhibitors is varied between the different plasmepsins, but one observation that seems to be consistent is that good experimental inhibitors were shown to interact with the plasmepsin active-site residues through a mixture of hydrophobic and polar interactions (Table 2 and Figure 9). This observation was also highlighted by the fact that compounds that only bound through hydrophobic interactions were generally poorer inhibitors than those with mixed interactions. This work leads to the idea that only crystallographic studies will give a clear understanding of the various conformational modes of binding of these peptidomimetic inhibitors.

As observed from both the combinatorial substrate analyses and the inhibition studies, the specificities of the malarial aspartic peptidases share common characteristics. Future combinatorial libraries could incorporate unnatural amino acids at the points of complexity to elucidate more unique determinants of specificity. Similarly, the use of various transition-state mimetics, such as ketomethylamine [-CO-CH_2-NH-], hydroxyethylamine [-CHOH-CH_2-NH-], and hydroxyethylene [-CHOH-CH_2-], can be incorporated between the P1 and P1′ residues of future inhibitory compounds (*48*). Last, it would be ideal to identify small nonpeptidyl compounds that inhibit the plasmepsins, because large compounds often have difficulty crossing plasma membranes and obtaining access to the parasitic food vacuole.

ACKNOWLEDGMENT

The authors thank Charlie Craik and Debbie Dauber for helpful discussions.

REFERENCES

1. World malaria situation in 1994. Part I. Population at risk. (1997) in *Weekly Epidemiological Record*, Vol. 72, pp 269−274.
2. Francis, S. E., Sullivan, D. J., Jr., and Goldberg, D. E. (1997) Hemoglobin metabolism in the malaria parasite *Plasmodium falciparum*, *Annu. Rev. Microbiol. 51*, 97−123.
3. Goldberg, D. E., Slater, A. F., Cerami, A., and Henderson, G. B. (1990) Hemoglobin degradation in the malaria parasite *Plasmodium falciparum*: An ordered process in a unique organelle, *Proc. Natl. Acad. Sci. U.S.A. 87*, 2931−2935.
4. Coombs, G. H., Goldberg, D. E., Klemba, M., Berry, C., Kay, J., and Mottram, J. C. (2001) Aspartic proteases of *Plasmodium falciparum* and other parasitic protozoa as drug targets, *Trends Parasitol. 17*, 532−537.
5. Goldberg, D. E., Slater, A. F., Beavis, R., Chait, B., Cerami, A., and Henderson, G. B. (1991) Hemoglobin degradation in the human malaria pathogen *Plasmodium falciparum*: A catabolic pathway initiated by a specific aspartic protease, *J. Exp. Med. 173*, 961−969.
6. Klemba, M., and Goldberg, D. E. (2002) Biological roles of proteases in parasitic protozoa, *Annu. Rev. Biochem. 71*, 275−305.
7. Shenai, B. R., Sijwali, P. S., Singh, A., and Rosenthal, P. J. (2000) Characterization of native and recombinant falcipain-2, a principal trophozoite cysteine protease and essential hemoglobinase of *Plasmodium falciparum*, *J. Biol. Chem. 275*, 29000−29010.
8. Murata, C. E., and Goldberg, D. E. (2003) *Plasmodium falciparum* falcilysin−A metalloprotease with dual specificity, *J. Biol. Chem. 278*, 38022−38028.
9. Eggleson, K. K., Duffin, K. L., and Goldberg, D. E. (1999) Identification and characterization of falcilysin, a metallopeptidase involved in hemoglobin catabolism within the malaria parasite *Plasmodium falciparum*, *J. Biol. Chem. 274*, 32411−32417.
10. Francis, S. E., Gluzman, I. Y., Oksman, A., Knickerbocker, A., Mueller, R., Bryant, M. L., Sherman, D. R., Russell, D. G., and Goldberg, D. E. (1994) Molecular characterization and inhibition of a *Plasmodium falciparum* aspartic hemoglobinase, *EMBO J. 13*, 306−317.
11. Moon, R. P., Tyas, L., Certa, U., Rupp, K., Bur, D., Jacquet, C., Matile, H., Loetscher, H., Grueninger-Leitch, F., Kay, J., Dunn, B. M., Berry, C., and Ridley, R. G. (1997) Expression and characterisation of plasmepsin I from *Plasmodium falciparum*, *Eur. J. Biochem. 244*, 552−560.
12. Li, T., Yowell, C. A., Beyer, B. B., Hong, S.-W., Westling, J., Lam, M. T., Dunn, B. M., and Dame, J. B. (2004) Recombinant expression and enzymatic subsite characterization of plasmepsin 4 from the four *Plasmodium* species infecting man, *Mol. Biochem. Parasitol. 135*, 101−109.
13. Pinilla, C., Appel, J. R., Blanc, P., and Houghten, R. A. (1992) Rapid identification of high affinity peptide ligands using positional scanning synthetic peptide combinatorial libraries, *BioTechniques 13*, 901−905.
14. Dooley, C. T., and Houghten, R. A. (1993) The use of positional scanning synthetic peptide combinatorial libraries for the rapid determination of opioid receptor ligands, *Life Sci. 52*, 1509−1517.
15. Harris, J. L., Backes, B. J., Leonetti, F., Mahrus, S., Ellman, J. A., and Craik, C. S. (2000) Rapid and general profiling of protease specificity by using combinatorial fluorogenic substrate libraries, *Proc. Natl. Acad. Sci. U.S.A. 97*, 7754−7759.
16. Backes, B. J., Harris, J. L., Leonetti, F., Craik, C. S., and Ellman, J. A. (2000) Synthesis of positional-scanning libraries of fluorogenic peptide substrates to define the extended substrate specificity of plasmin and thrombin, *Nat. Biotechnol. 18*, 187−193.
17. Dunn, B. M., and Hung, S. H. (2000) The two sides of enzyme−substrate specificity: Lessons from the aspartic proteinases, *Biochim. Biophys. Acta 1477*, 231−240.
18. Silva, A. M., Lee, A. Y., Gulnik, S. V., Maier, P., Collins, J., Bhat, T. N., Collins, P. J., Cachau, R. E., Luker, K. E., Gluzman, I. Y., Francis, S. E., Oksman, A., Goldberg, D. E., and Erickson, J. W. (1996) Structure and inhibition of plasmepsin II, a hemoglobin-degrading enzyme from *Plasmodium falciparum*, *Proc. Natl. Acad. Sci. U.S.A. 93*, 10034−10039.
19. Asojo, O. A., Gulnik, S. V., Afonina, E., Yu, B., Ellman, J. A., Haque, T. S., and Silva, A. M. (2003) Novel uncomplexed and complexed structures of plasmepsin II, an aspartic protease from *Plasmodium falciparum*, *J. Mol. Biol. 327*, 173−181.
20. Asojo, O. A., Afonina, E., Gulnik, S. V., Yu, B., Erickson, J. W., Randad, R., Medjahed, D., and Silva, A. M. (2002) Structures of Ser205 mutant plasmepsin II from *Plasmodium falciparum* at 1.8 Å in complex with the inhibitors rs367 and rs370, *Acta Crystallogr., Sect. D 58* (part 12), 2001−2008.
21. Westling, J., Yowell, C. A., Majer, P., Erickson, J. W., Dame, J. B., and Dunn, B. M. (1997) *Plasmodium falciparum*, *P. vivax*, and *P. malariae*: A comparison of the active site properties of plasmepsins cloned and expressed from three different species of the malaria parasite, *Exp. Parasitol. 87*, 185−193.
22. Dame, J. B., Reddy, G. R., Yowell, C. A., Dunn, B. M., Kay, J., and Berry, C. Sequence, expression, and modeled structure of an aspartic proteinase from the human malaria parasite *Plasmodium falciparum*, *Mol. Biochem. Parasitol. 64*, 177−190.

23. Hill, J., Tyas, L., Phylip, L. H., Kay, J., Dunn, B. M., and Berry, C. (1994) High level expression and characterisation of Plasmepsin II, an aspartic proteinase from *Plasmodium falciparum*, *FEBS Lett. 352*, 155−158.
24. Beyer, B. M., and Dunn, B. M. (1996) Self-activation of recombinant human lysosomal procathepsin D at a newly engineered cleavage junction, "short" pseudocathepsin D, *J. Biol. Chem. 271*, 15590−15596.
25. Beyer, B. B., Goldfarb, N. E., and Dunn, B. M. (2003) Expression, purification, and characterization of aspartic endopeptidases: *Plasmodium* plasmepsins and "short" recombinant human pseudocathepsin, in *Current Protocols in Protein Science* (Coligan, J. E., Dunn, B. M., Speicher, D. W., and Wingfield, P. T., Eds.) pp 21.14.1−21.14.24, John Wiley and Sons, New York.
26. Pennington, M. W. (1994) Solid-phase synthesis of peptides containing the CH2NH reduced bond surrogate, *Methods Mol. Biol. 35*, 241−247.
27. Skrbec, D., and Romeo, D. (2002) Inhibition of *Candida albicans* secreted aspartic protease by a novel series of peptidomimetics, also active on the HIV-1 protease, *Biochem. Biophys. Res. Commun. 297*, 1350−1353.
28. Cooper, H. J., Hudgins, R. R., Hakansson, K., and Marshall, A. G. (2002) Characterization of amino acid side chain losses in electron capture dissociation, *J. Am. Soc. Mass Spectrom. 13*, 241−249.
29. Wee, S., O'Hair, R. A., and McFadyen, W. D. (2002) Side-chain radical losses from radical cations allows distinction of leucine and isoleucine residues in the isomeric peptides Gly-XXX-Arg, *Rapid Commun. Mass Spectrom. 16*, 884−890.
30. Beyer, B. M., and Dunn, B. M. (1998) Prime region subsite specificity characterization of human cathepsin D: The dominant role of position 128, *Protein Sci. 7*, 88−95.
31. Westling, J., Cipullo, P., Hung, S. H., Saft, H., Dame, J. B., and Dunn, B. M. (1999) Active site specificity of plasmepsin II, *Protein Sci. 8*, 2001−2009.
32. Hill, J., Montgomery, D. S., and Kay, J. (1993) Human cathepsin E produced in *E. coli*, *FEBS Lett. 326*, 101−104.
33. Dunn, B. M., Scarborough, P. E., Davenport, R., and Swietnicki, W. (1994) Analysis of proteinase specificity by studies of peptide substrates. The use of UV and fluorescence spectroscopy to quantitate rates of enzymatic cleavage, *Methods Mol. Biol. 36*, 225−243.
34. Morrison, J. F. (1969) Kinetics of the reversible inhibition of enzyme-catalysed reactions by tight-binding inhibitors, *Biochim. Biophys. Acta 185*, 269−286.
35. Peitsh, M. C. (1995) *BioTechniques 13*, 658−660.
36. Peitsh, M. C. (1996) *Biochem. Soc. Trans. 24*, 274−279.
37. *SYBYL* (2002) Tripos Associates, St. Louis, MO.
38. Morris, G. M., Goodsell, D. S., Halliday, R. S., Huey, R., Hart, W. E., Belew, R. K., and Olson, A. J. (1998) Automated docking using a Lamarkian Genetic algorithm and empirical binding free energy function, *J. Comput. Chem. 19*, 1639−1662.
39. Osterberg, F., Morris, G. M., Sanner, M. F., Olson, A. J., and Goodsell, D. S. (2002) Automated docking to multiple target structures: Incorporation of protein mobility and structural water heterogeneity in AutoDock, *Proteins 46*, 34−40.
40. Ji, H., Li, H., Flinspach, M., Poulos, T. L., and Silverman, R. B. (2003) Computer modeling of selective regions in the active site of nitric oxide synthases: Implication for the design of isoform-selective inhibitors, *J. Med. Chem. 46*, 5700−5711.
41. Fruton, J. S. (1970) The specificity and mechanism of pepsin action, *Adv. Enzymol. Relat. Areas Mol. Biol. 33*, 401−443.
42. Powers, J. C., Harley, A. D., and Myers, D. V. (1977) Subsite specificity of porcine pepsin, *Adv. Exp. Med. Biol. 95*, 141−157.
43. Scarborough, P. E., Guruprasad, K., Topham, C., Richo, G. R., Conner, G. E., Blundell, T. L., and Dunn, B. M. (1993) Exploration of subsite binding specificity of human cathepsin D through kinetics and rule-based molecular modeling, *Protein Sci. 2*, 264−276.
44. Banerjee, R., Liu, J., Beatty, W., Pelosof, L., Klemba, M., and Goldberg, D. E. (2002) Four plasmepsins are active in the *Plasmodium falciparum* food vacuole, including a protease with an active-site histidine, *Proc. Natl. Acad. Sci. U.S.A. 99*, 990−995.
45. Luker, K. E., Francis, S. E., Gluzman, I. Y., and Goldberg, D. E. (1996) Kinetic analysis of plasmepsins I and II aspartic proteases of the *Plasmodium falciparum* digestive vacuole, *Mol. Biochem. Parasitol. 79*, 71−78.
46. Gardner, M. J., Hall, N., Fung, E., White, O., Berriman, M., Hyman, R. W., Carlton, J. M., Pain, A., Nelson, K. E., Bowman, S., Paulsen, I. T., James, K., Eisen, J. A., Rutherford, K., Salzberg, S. L., Craig, A., Kyes, S., Chan, M. S., Nene, V., Shallom, S. J., Suh, B., Peterson, J., Angiuoli, S., Pertea, M., Allen, J., Selengut, J., Haft, D., Mather, M. W., Vaidya, A. B., Martin, D. M., Fairlamb, A. H., Fraunholz, M. J., Roos, D. S., Ralph, S. A., McFadden, G. I., Cummings, L. M., Subramanian, G. M., Mungall, C., Venter, J. C., Carucci, D. J., Hoffman, S. L., Newbold, C., Davis, R. W., Fraser, C. M., and Barrell, B. (2002) Genome sequence of the human malaria parasite *Plasmodium falciparum*, *Nature 419*, 498−511.
47. Siripurkpong, P., Yuvaniyama, J., Wilairat, P., and Goldberg, D. E. (2002) Active site contribution to specificity of the aspartic proteases plasmepsins I and II, *J. Biol. Chem. 277*, 41009−41013.
48. Kay, J., and Dunn, B. M. (1992) Substrate specificity and inhibitors of aspartic proteinases, *Scand. J. Clin. Lab. Invest. 210*, 23−30.
49. Wallace, A. C., Laskowski, R. A., and Thornton, J. M. (1995) LIGPLOT: A program to generate schematic diagrams of protein−ligand interactions, *Protein Eng. 8*, 127−134.

BI047886U